Journal of Electroanalytical Chemistry 851 (2019) 113447

Contents lists available at ScienceDirect

Journal of Electroanalytical Chemistry

journal homepage: www.elsevier.com/locate/jelechem

Air-stable, high contrast solution-phase electrochromic device based on an A-D-A viologen derivative

Huan Ling [a,b], Xiaowen Wu [b], Ke Li [c], Fengyu Su [d,*], Yanqing Tian [b,*], Dan Luo [c], Yan Jun Liu [c,*], Xiao Wei Sun [c]

[a] School of Chemistry and Chemical Engineering, Harbin Institute of Technology, Harbin 150001, China
[b] Department of Materials Science and Engineering, Southern University of Science and Technology, Shenzhen 518055, China
[c] Department of Electrical and Electronic Engineering, Southern University of Science and Technology, Shenzhen 518055, China
[d] Academy for Advanced Interdisciplinary Studies, Southern University of Science and Technology, Shenzhen 518055, China

ARTICLE INFO

Article history:
Received 31 July 2019
Received in revised form 2 September 2019
Accepted 2 September 2019
Available online 03 September 2019

Keywords:
Electrochromic device
Air-stable
High contrast
A-D-A structure
Viologen

ABSTRACT

Electrochromic (EC) devices with reversible transmittance switching have promising prospects in the applications of photoelectric displays. Herein, a novel air-stable and high contrast solution-phase electrochromic device based on new viologen derivative (DPB) with A-D-A structure (A: acceptor; D: donor) was demonstrated. Devices possessed simple configuration of ITO/EC solution/ITO. Ferrocene and polycarbonate (PC) were selected as the complementary material and solvent, respectively. All of the fabrications and performance testing work were conducted in normal air condition. The DPB-based device showed deep magenta color in colored state and exhibited high optical contrast of ΔT of 72.2% (517 nm) and good coloration efficiency of 102.2 cm^2/C at 1.8 V. The device appeared only slight degradation of ΔT (ΔT = 69.6% or retained 96.7% of its initial ΔT after 5000 s constant switching) under the normal air atmosphere, which was even better than some reported well-packaged viologen-based solution ECDs. Additionally, the UV–vis reflective spectra were also conducted to assess the reflectance property of the devices. The reflectance peak (ΔR = 2.6%) and absorption peak matched accurately, which indicated that the new viologen derivative possesses the potential application in reflective electrochromic devices.

1. Introduction

With the advance of intelligent devices such as intelligent display screens and smart windows, a demand for the materials that respond quickly to temperature, transparency, light absorbance, and/or power is increasing. Electrochromic materials (ECMs) possess the features of reversible changes of their optical properties including absorbance, transmittance, reflectance and colors upon external electrical stimulus. Recently, electrochromic devices (ECDs), for unique and excellent performance, such as low power consumption, simple structures and ease of assembly, have been employed for diverse applications, ranging from intelligent modules [1,2], multiple color displays [3–5], and sensors [6–8] to reflective devices [9–11], flexible electronics [4,12–16] and energy-storage devices [17–26]. Electrochromic materials (ECMs) possess features of reversible changes of their optical properties including absorbance, transmittance, reflectance and colors upon giving external electrical stimulus. Conventionally, a typical electrochromic device possesses multilayers comprising of conductive substrates, electrochromic materials, an ion conductor and an ion storage film. In general, electrochromic devices can be divided into three configurations [27]: (1) solid device structure, which is similar to a sandwich with electrochromic layer and ion storage layer separated by an electrolyte film; (2) solution-phase device structure, which possess the electroactive solution or polymeric electrolyte for dissolving the ECMs and counter electrode components; and (3) a configuration, which has an intermediate structure between the above two types with partial soluble species dissolved in electrolytes [3]. Compared with the solid devices, ECDs with solution-phase configuration demonstrated the self-bleaching advantage that devices can revert to their original states in absence of applied voltage because electroactive spices can convert to the original state from edges of the two electrodes. In addition, it is more energy-saving and cheaper to assemble the solution-phase devices because of their simple device structures. Solution-phase devices also take less time to complete coloration and bleaching processes than optical-battery devices [28].

Among the electrochromic materials, viologens (4, 4′-bipyridyl salts) attract numerous studies for their high optical contrast, excellent coloration efficiency, and multiple colors through molecular design [6,29–33]. Viologens demonstrated three redox states: dication, radical cation, and neutral viologen. The colors of ECDs significantly depend on

---

[*] Corresponding authors.
E-mail addresses: fysu@sustech.edu.cn (F. Su), tianyq@sustech.edu.cn (Y. Tian), yjliu@sustech.edu.cn (Y.J. Liu).

https://doi.org/10.1016/j.jelechem.2019.113447

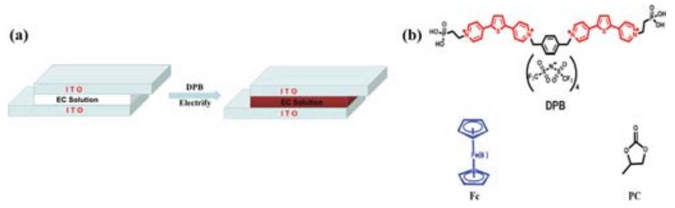

Fig. 1. Illustration of the ITO/EC solution/ITO configuration (a) and the newly synthesized viologen derivative (DPB) with ferrocene and propylene carbonate in EC solution (b).

the substituents bonding to nitrogen atoms on bipyridyl [21,29,30,34–36]. Normally, the dication form is colorless and the radical cation specie plays a dominating role in coloration process because of its high molar absorption coefficient (ε) [28]. Remarkably, the radical cation species of viologen demonstrates good solubility and acceptable stability in the solution or gel with suitable electron stimulate. Owing to these unique properties, viologens as the electrochromic materials were widely used in solution-phase or gel-phase ECDs. For examples, Mortimer et al. reported a novel methyl viologen-based color-reinforcing solution-phase ECD with ruthenium purple as the counter electrode material. By using this simple device construction, intense purple color and comparable response time were obtained [37]. Alesanco et al. presented a 1-alkyl-1′-aryl asymmetric viologen-based ECD, which showed transparent-to-black/gray color changes with good cyclability and high optical contrast [38]. It is noticeable that the efforts on viologen-based redox ionic liquids (RILs) are emerging recently [4,28,39–41]. Popularly, viologen-based RILs and ferrocene were served as cathode and anode materials, respectively, the special case was a novel bonding ferrocene-viologen ionic liquid [42]. The performance of RILs devices significantly depends on the compositions of the ionic liquids. However, most viologens in RILs reported so far were general molecules with regular modification of the alkyl chains bonding to the bipyridyl. Considering the great potentials for further modification of the bipyridyl derivatives, exploration of new viologen derivatives is necessary. What's more, most ionic liquids are sensitive to moisture. Water and oxygen have huge effects on the performance of RILs. As a result, significant efforts and a lot of time are needed to assemble the complex devices. Conversely, Nagamura et al. [30] reported a hyperbranched polymer with viologen units based EC windows. The display exhibited excellent electrochromic performance even if no active sealing work was conducted owing to the radical cation species, which indicates that ECDs are able to exhibit good electrochromism without strict sealing work if the radical cation species is stable enough.

In this work, a novel viologen derivative (DPB) was synthesized (Fig. 1) and used as the EC material in solution-phase ECD. The chromophore in DPB was to explore the capability of adjusting the bipyridyl conjugation by inserting a thiophene unit between the two pyridyl units in solution-phase ECD. This A-D-A structure not only stabilized the radical cation that played a dominate role in colored state, but also narrowed the band gap of π-π*, which resulted in an obvious bathochromic shift when comparing to the similar viologen without thiophene moiety [43]. We have noticed that phosphate groups were utilized to anchor to TiO_2 nanoparticles among a series of viologen-based solid ECDs with high stability [38,44,45]. However, viologens bearing phosphates had not been utilized as EC materials in other types of ECDs. In addition, Sui et al. reported a zwitterionic viologen bearing carboxylate groups, in which the viologen radical formation and quenching were dominated by reversible electron transfer between the carboxylate groups and viologen moiety related to intermolecular donor-acceptor contacts. Similarly, Li et al. [46] combined the methyl viologen with graphene quantum dots through strong inter-molecular forces using electrostatic interactions between carboxylate groups and viologen. These studies demonstrated that the carboxylate group was served as potential electron donor during redox process. Therefore, by introducing phosphate groups in viologens may not only contribute to the electron transfer between phosphate groups and viologens, but also stabilize the viologen radicals. Finally, in order to improve the solubility and the ionic conductivity of viologen in organic solvent, Lithium bis(trifluoromethanesulphonyl)imide (TFSI) was selected as counter

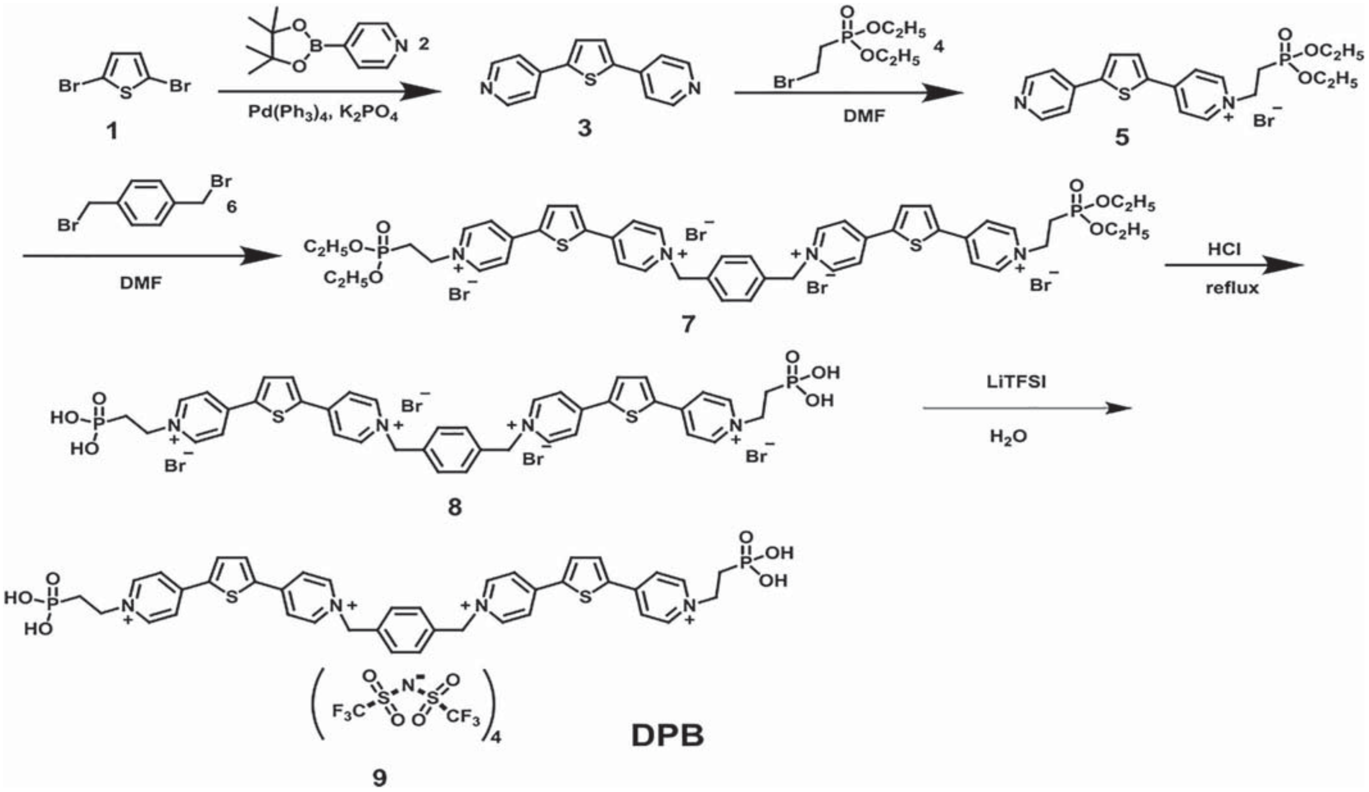

Scheme 1. Synthetic route of 4,4′-(((1,4-phenylenebis(methylene))bis(pyridine-1-ium-1,4-diyl)) bis(thiophene-5,2-diyl))bis(1-(2-phosphonoethyl)pyridine-1-ium) tetra-TFSI$^-$ (DPB).

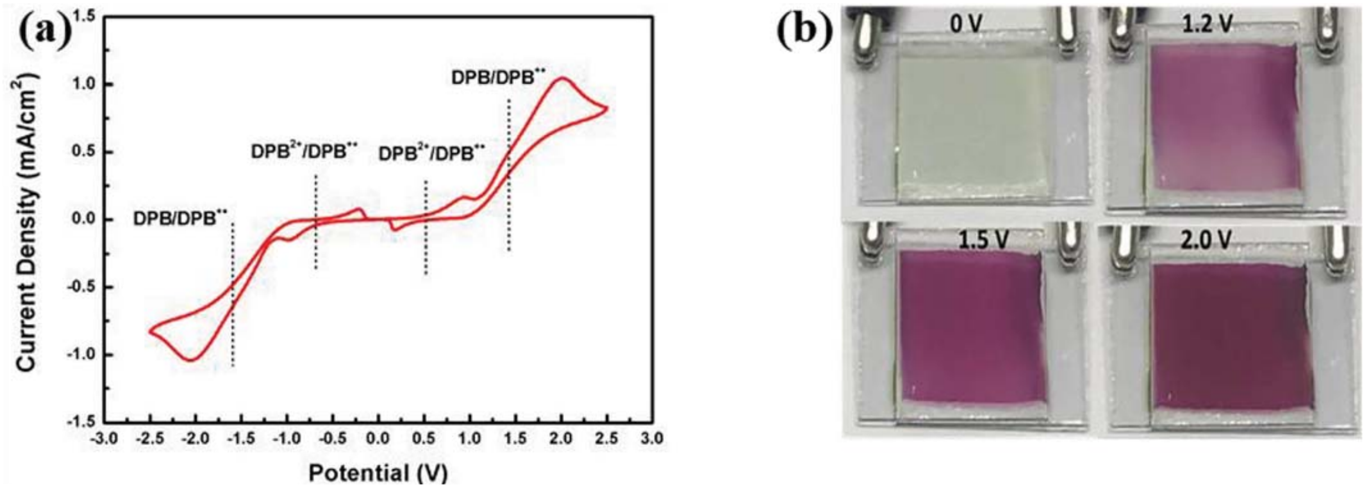

Fig. 2. (a) Cyclic voltammograms of ECD based on DPB at a scan rate of 0.1 V/s between −2.5 and 2.5 V at room temperature. (b) Photographs of DPB-based ECD with different applied voltages. The choice of 0 V was used to show the neutral state of device; the choice of 1.2 V aimed to exhibit the first colored state of device; the selection of 1.5 V was to describe darker color in coloring process; the choice of 2.0 V was for demonstrating the darkest color in coloring process.

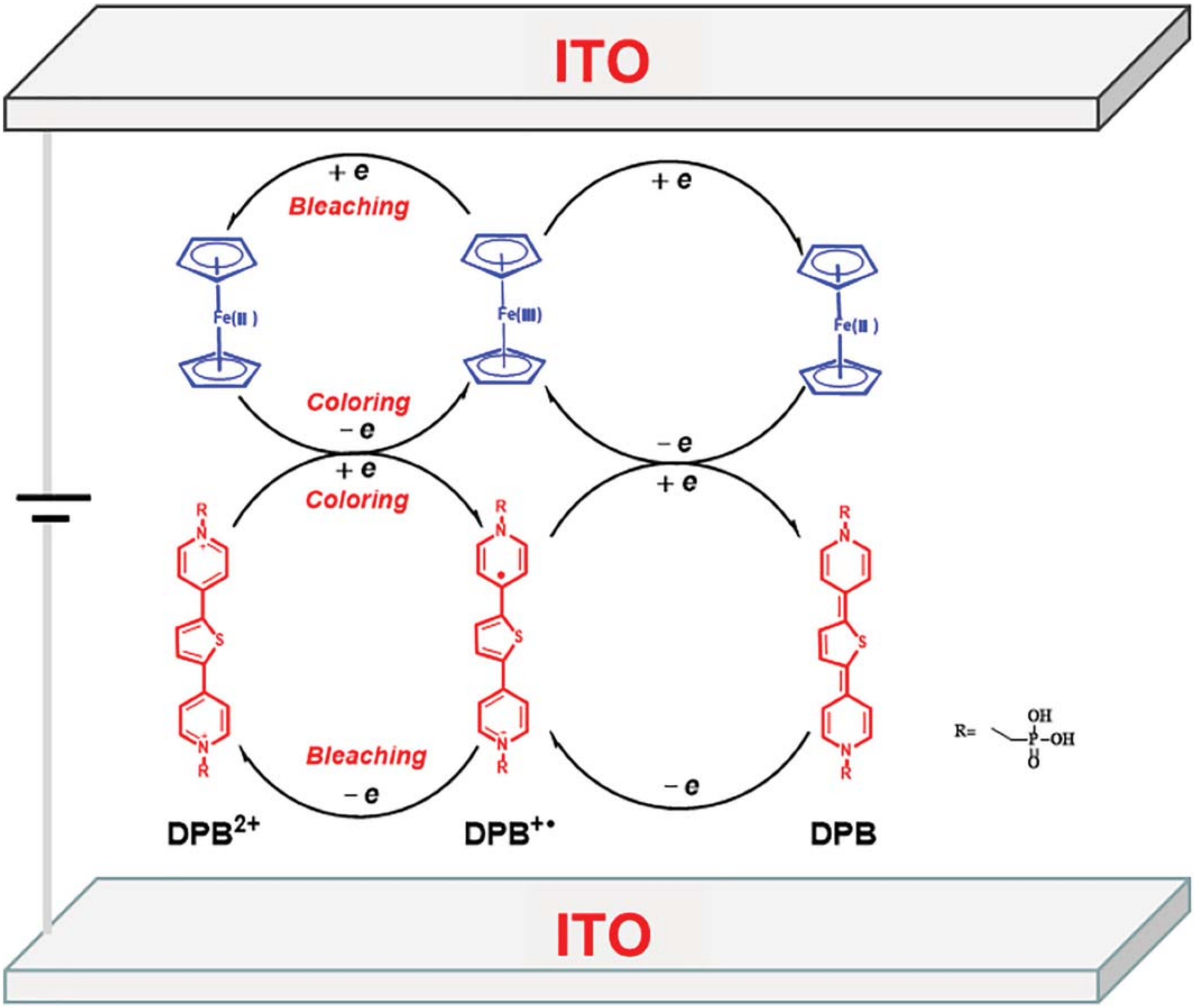

Fig. 3. Proposed redox mechanism for DPB-based ECDs.

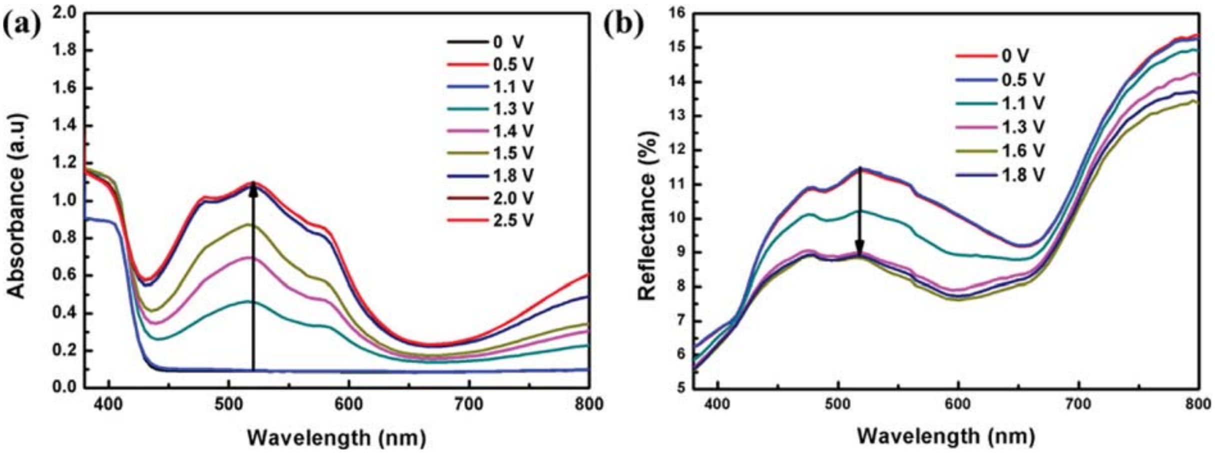

Fig. 4. UV–vis absorption (a) and reflectance (b) spectra of the DPB-based ECD with different applied voltages.

anions. Several candidates for the anode species were assessed. The well-known ferrocene was selected as complementary material for its good solubility, low operating voltage and excellent chemical stability when compared with other counter materials (Fig. S1). Device was fabricated using simple configuration by inserting the layer of electroactive solution consisting of DPB and ferrocene between the two pieces of ITO glasses (Fig. 1). Eventually, DPB-based device successfully demonstrated excellent electrochromic properties although whole device performance was evaluated in normal air condition.

2. Experimental

2.1. Materials and instruments

Commercially available raw chemicals were used without further purification. 4, 4′-Bipyridine was purchased from J&K Chemical (Beijing, China). Diethyl 2-bromoethylphosphonate was ordered from Energy Chemical (Shanghai, China). 1,4-Bis(bromomethyl) benzene was from TCI (Shanghai, China). HCl was purchased from Damao Chemical Ltd. (Shanghai, China). 4-Pyridylboronic acid pinacol ester was obtained from Nine Ding Chemical Ltd. (Shanghai, China). Potassium phosphate was ordered from Macklin (Shanghai, China). Lithium bis(trifluoromethanesulphonyl)imide (TFSI) was purchased from Aladdin (Shanghai, China). 2, 5-Dibromothiophene and 3, 4-ethylenedioxythiophene were purchased from Heowns (Tianjin, China). All solvents were purchased from XiLong Scientific (Guangzhou, China). ITO glasses were purchased from NSG Group (Osaka, Japan).

Nuclear Magnetic Resonance (NMR) spectra were acquired through NMR (Bruker 400M; 400 MHz for ^{1}H NMR, 101 MHz for ^{13}C NMR, Bremen). Mass spectra were obtained by HRMS (Q-Exactive, Massachusetts). The electrochemical properties were characterized by electrochemical workstation (Ametek Parstat 3000A-DX, Berwyn). The optical properties were measured by UV–vis spectrophotometer (L6020365, Waltham) and Colorimeter (CHN Spec CS-820, Guangzhou) combined with Waveform Generator (Rigol DG4102 Function/Arbitrary, Suzhou). A digital camera was used to record the photographs of devices.

2.2. Materials synthesis

Scheme 1 gave the synthetic route of DPB.

The details of synthesis route and characterization were placed in Supporting information.

2.3. Fabrication of ECDs

First, small frame shape of parafilm was put on the edges of an ITO glass and served as a spacer; and then another ITO glass was put on the top of this ITO glass with the parafilm. The two ITO glasses were pressed together tightly through a subpress, leaving a 70 μm gap. The

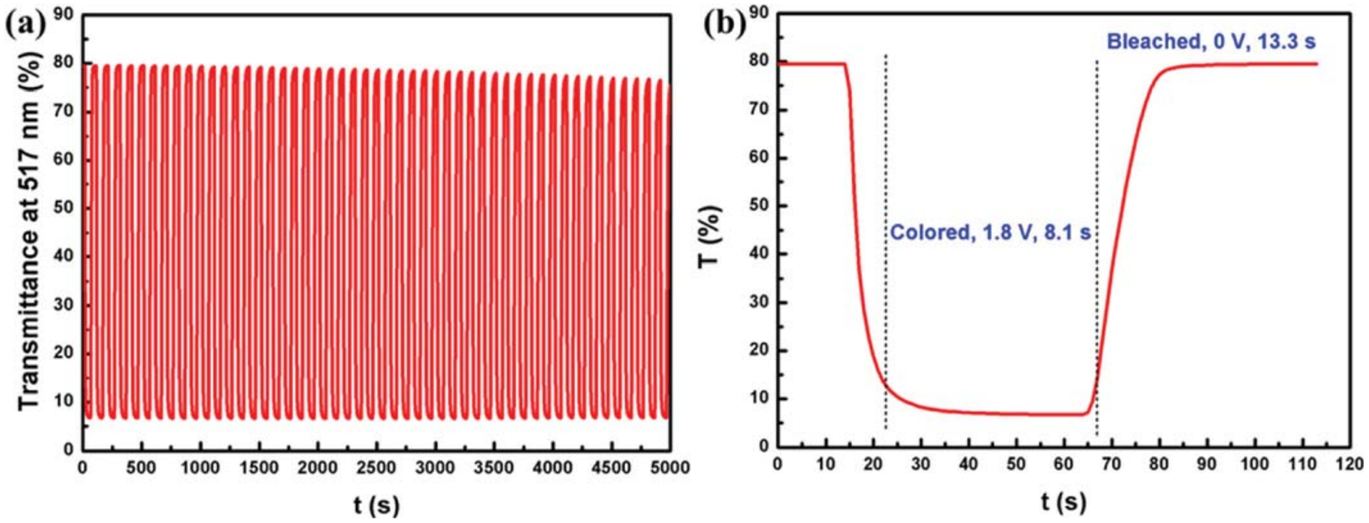

Fig. 5. UV–vis transmittance changes (a) at 517 nm for the DPB-based ECD and response time (b) for achieving 90% conversion. The voltage applied were 1.8 V (50 s) and 0 V (50 s).

Table 1
Performance of other viologen-ferrocene system solution phase ECDs.

Compounds	ΔT (%)	Change in ΔT% after 4000 s work time
1-(2-Methoxy-2-oxoethyl)-[4,4′-bipyridin]-1-ium [48]	35.9	7.9
1-(2-Ethoxy-2-oxoethyl)-[4,4′-bipyridin]-1-ium [48]	31.4	21.4
1-(2-Butoxy-2-oxoethyl)-[4,4′-bipyridin]-1-ium [48]	17.5	14.5
1-(2-(Tert-butoxy)-2-oxoethyl)-[4,4′-bipyridin]-1-ium [48]	15.3	11.5
1,1′-Bis(2-methoxy-2-oxoethyl)-[4,4′-bipyridine]-1,1′-diium [48]	35.2	16.2
1,1′-Bis(2-ethoxy-2-oxoethyl)-[4,4′-bipyridine]-1,1′-diium [48]	32.2	18.0
1,1′-Bis(2-butoxy-2-oxoethyl)-[4,4′-bipyridine]-1,1′-diium [48]	42.5	15.0
1,1′-Bis (2-(tert-butoxy)-2-oxoethyl)-[4,4′-bipyridine]-1,1′-diium [48]	35.0	30.0
DPB (this work)	72.2	2.6 (5000 s)

EC solution containing 0.01 M DPB and 0.027 M ferrocene in PC was injected into the gap without any other adhesive sealing.

3. Results and discussion

3.1. Electrochemical properties

To evaluate the performance of ECDs, cyclic voltammetry (CV) in a two-electrode system was utilized to characterize the electrochemical properties. The cyclic voltammograms were carried out at a scan rate of 0.1 V/s between −2.5 V and 2.5 V. As shown in Fig. 2a, two pairs of redox peaks in the cyclic voltammetry were observed, which were attributed to the chromophore of DPB. And it is a remarkable fact that each cyclic voltammetry curve was almost symmetrical, which can be attributed to the symmetrical structure of the solution-phase ECDs. When voltage was below 0.6 V, the current density was close to zero, indicating that no redox reactions occurred at this point. The anodic and cathodic peaks of Fc^+/Fc could not be observed in the CV curve, which would be possibly overlapped by the first redox couple of $DPB^{2+}/DPB^{+\bullet}$. The first cathodic peak was observed at -0.98 V. The rational explanation for this observation is that the DPB^{2+} was reduced to $DPB^{+\bullet}$ upon applying an appropriate voltage. Anodic peak at -0.43 V was ascribed to the oxidation conversion of $DPB^{+\bullet}$ to the DPB^{2+} dication salts. Then, the chromophore with radical cations of $DPB^{+\bullet}$ got electrons and generated full reduced state of DPB^0 species and the corresponding cathodic peak of $DPB^{+\bullet}/DPB^0$ was detected at −2.0 V. Meanwhile, the device turned magenta from slight yellow as shown in Fig. 2b. Hence, similar to the common viologens, the redox mechanism of DPB was proposed in Fig. 3. As-fabricated devices without any voltage applied exhibited a pale yellow color due to the dissolution of ferrocene. Normally, various N-substituent groups in the bipyridyl moieties result in different colors on ECDs [47]. With increase of the stimulating voltage, the color of device turned darker and darker immediately, which confirmed a dramatic transformation to the colored state from transparent state. Devices possess the ability of self-erasing with the exposure of electroactive materials to air and moisture repeatedly once the electrical power was cut off. In addition, more viologen molecules leaded to darker color (Fig. S2). When compared to another similar viologen-based ECD (Fig. S3) with blue color in colored state reported by Xu et al. [43], we can conclude that DPB chromophore with acceptor-donor-acceptor molecular structure can narrow the band gap of radical cations after introducing the thiophene ring between the two pyridine units of the normal viologens.

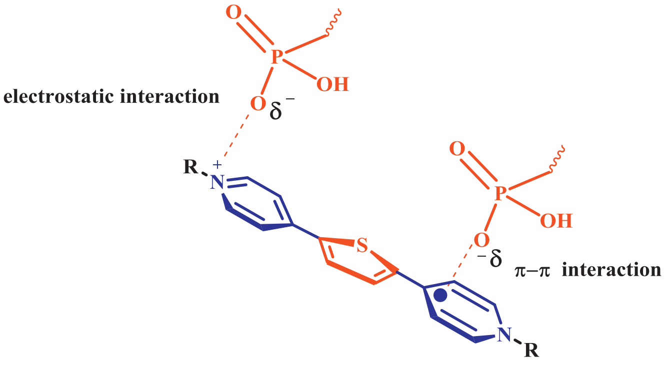

Fig. 6. Proposed interactions between phosphate groups and viologen.

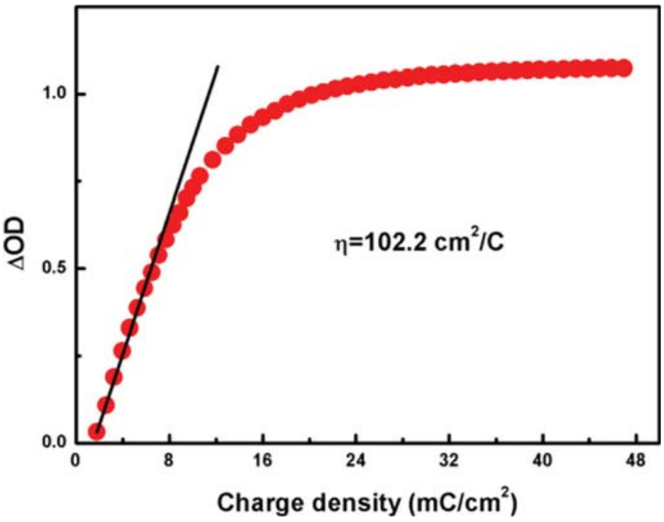

Fig. 7. Optical density (OD) versus charge density at 517 nm of the DPB-based ECD.

3.2. Spectroelectrochemistry properties

Fig. 4a gave the UV–vis absorption spectra of ECD with different applied voltages. The device was highly transparent at bleached state with a transmittance of approximately 80% in the range from 450 nm to 800 nm (Fig. S4). The device exhibited no obvious absorbance change when the applied voltage was below 1.1 V. Broad absorption peak was observed at 517 nm with the voltage of 1.3 V. Subsequently, the absorbance increased dramatically along with the increase of the applied voltages and the ECD turned into deep magenta as shown in Fig. 2b. Reasonable explanation for this transformation would be the higher concentration of $DPB^{+\bullet}$ under the stronger electron stimulating. Remarkably, the device was able to exhibit deep magenta at 3 V when

Table 2
The comparison of color efficiency performance of a few typical solution-phase EC devices with viologen-ferrocene.

Viologens	λ_{max}	Color efficiency (cm^2/C)	Ref
NV[a]	605	36.2	40
BHV[b]	540	91.4	41
$FcC_{11}VC_1$[c]	550	70	42
HV[d]	605	78	51
MOV[e]	536	247.5	48
BMOV[f]	597	268.5	48
DPB	517	102.2	This work

All the compounds' structures were given in Fig. S6.

[a] 1,1′-Nonyl-[4,4′-bipyridine]-1,1′-diium ditetrafluoroborate.

[b] 1-Butyl-1′-heptyl-[4,4′-bipyridine]-1,1′-diium dibis(trifluoromethylsulfonyl)imide.

[c] Structure was given in Fig. S6.

[d] 1,1′-Diheptyl-[4,4′-bipyridine]-1,1′-diium dibis(trifluoromethylsulfonyl)imide.

[e] 1-(2-Methoxy-2-oxoethyl)-[4,4′-bipyridin]-1-ium bromide.

[f] 1,1′-Bis(2-methoxy-2-oxoethyl)-[4,4′-bipyridine]-1,1′-diium dibromide.

Table 3
Colorimetric parameters for TMP-based ECD in different redox states.

Redox states for ECD	L*	a*	b*
DPB-c[1]	30.8	19.42	2.03
DPB-b[2]	83.86	−6.34	11.42

[1] c represents for colored state.
[2] b represents for bleached state.

exposed to the air for several mins (Fig. S5). In order to study the reflective performance of ECD, UV–vis reflectance spectra under different applied voltages were recorded and depicted in Fig. 4b. Decreased reflectance was observed for the ECD with the increase of applied voltages. 2.6% of maximum reflectance contrast at 517 nm was obtained. And the specific peaks in 517 nm matched very well with the absorption peaks of the device. The applied electric field has similar effects on the transmittance and reflectivity of the same device in the visible range, which suggested that the investigated ECDs can be applied as promising reflective electrochromic devices.

3.3. Stability and switching properties of the ECD

Cyclic stability and response time are significant factors to estimate the performance of ECDs especially when the ECMs were exposed to the air. To acquire maximal ΔT and fast response time, the applied voltage on device was fixed at relatively high voltage of 1.8 V. The initial ΔT of the device was 72.2% at 517 nm. And after an operating time of 5000 s, slight degradation (loss 3.3% of initial ΔT, 69.6% of ΔT was obtained) was observed as shown in Fig. 5a. Compared to other viologen-based solution-phase ECDs, DPB-based ECDs possess much better optical contrast and higher stability as shown in Table 1.

Fig. 5b showed that the time required for achieving 90% of transmittance contrast was 8.1 s for coloring process and 13.3 s for bleaching process. The reason for the long response time was that the large

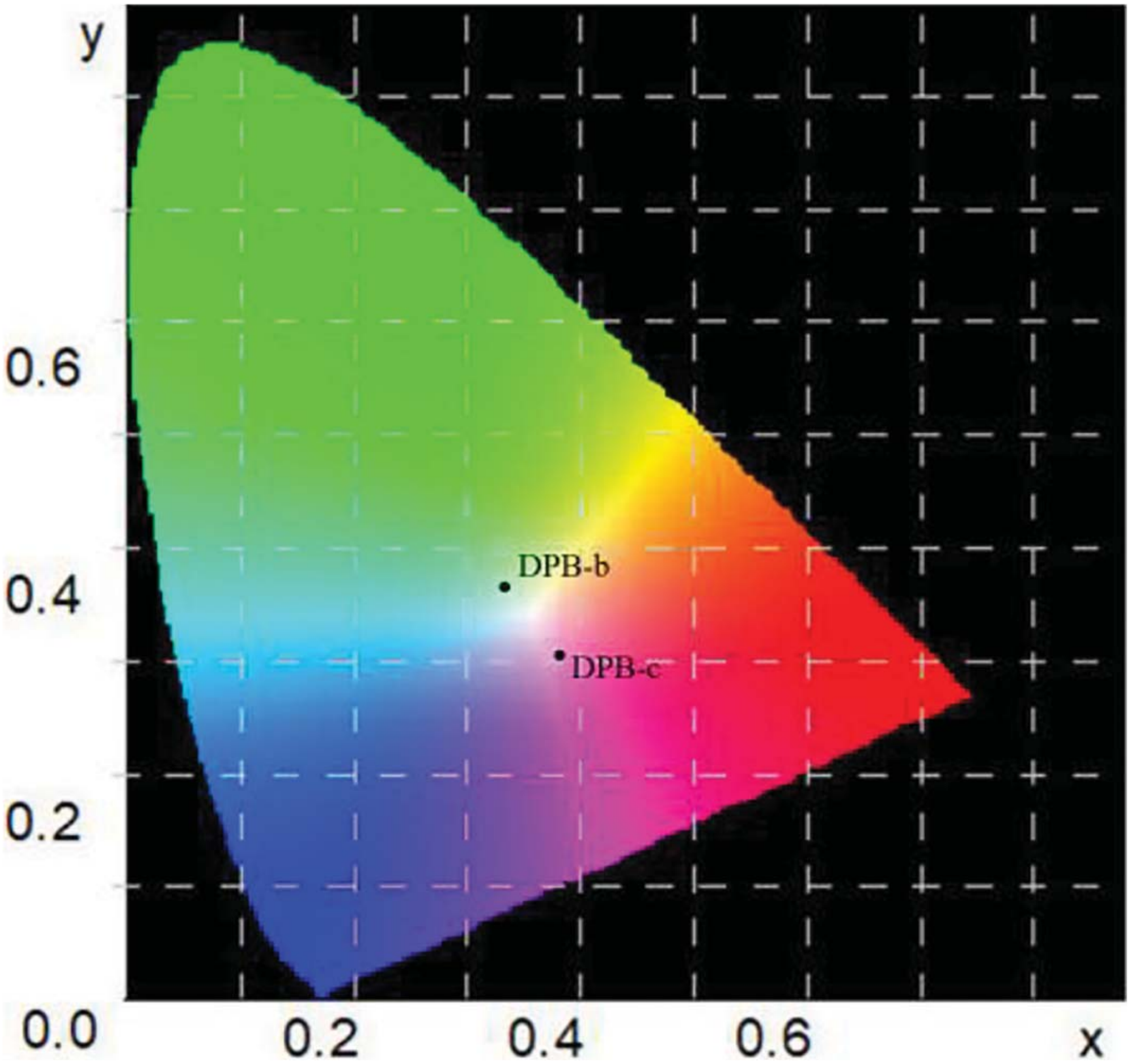

Fig. 8. Colorimetry of ECDs in the colored and bleached state.

$[TFSI]^-$ ions cost more time to diffuse and the large counter anions will be easily trapped on the electrode surface [49]. Furthermore, the transmittance of device exhibited no degradation in colored state after constant switching, which indicated high stability of viologen cation. This excellent stability might be attributed to the introducing of thiophene ring, and possibly, the π-π interactions and electrostatic interactions between phosphate groups and viologen moiety as shown in Fig. 6.

3.4. Coloration efficiency

One of the significant characteristic parameters for evaluating ECDs performance is coloration efficiency (η). The η is defined in Eq. (2) [50].

$$\eta = \Delta OD/\Delta Q = \log (T_b - T_c)/\Delta Q \tag{2}$$

where ΔOD refers to the change of optical density, T_b and T_c are the transmittance for bleached and colored state at a specific wavelength. ΔQ represents the amount of charge transfer per unit area in accordance with optical contrast. The value of η can estimate the ability to acquire high optical contrast with low injected charge for ECDs. As showed in Fig. 7, η was calculated from the fitted slope of the linear regime with the function of ΔOD as the Y axis, ΔQ as the X axis. The coloration efficiency (η) for the device was calculated to be 102.2 cm^2/C (at 1.8 V), which indicated the device exhibited excellent coloration performance compared with other viologen-ferrocene electrochromic devices. Lu et al. combined viologen with ferrocene to make polymeric ionic liquids and got a 38.6 cm^2/C of coloration efficiency [40]. Moon et al. reported a viologen-dimethyl ferrocene (DMFc) gel ECD which achieved 78 cm^2/C [51]. Murakami et al. exhibited a novel viologen-ferrocene linked ECM with a η of 70 cm^2/C (Fig. S6) [42]. Hironobu et al. recently demonstrated a viologen-based redox-active ionic liquid ECD with an efficiency of 91.4 cm^2/C [41]. Fu et al. reported a series of ester groups-modified viologen that exhibited higher CE (>110 cm^2/C) value than DPB. Nevertheless, those devices' stability was extremely poor [48]. By comparison with other devices (Table 2), it was found that the DPB-based device has a good balance of coloration efficiency and stability.

3.5. Colorimetric properties of ECDs

For characterizing the colors of DPB-based ECD at different states, CIE system was utilized to obtain the chromaticity values. In the CIE system, L* is for the lightness; a* and b* are for the green–red and blue–yellow color components, respectively. Colorimetric data L*, a* and b* were listed in Table 3, values for the DPB-based ECD at bleached state were 83.86, −6.34 and 11.42, respectively. The high values of L* indicate that ECD appear near transparent without electrical stimulation. Subsequently, values are 30.8, 19.42 and 2.03, respectively in colored state. For DPB-based ECD, the dramatic decrease of value L* confirmed that transmittance had dropped sharply. The large numerical difference represented that ECD possess satisfactory coloration performance. In addition, the value of a* transferred from −6.34 to 19.42 indicated that the device had turned from yellow to magenta color (Fig. 8).

4. Conclusion

In this study, we have successfully fabricated a novel A-D-A viologen (DPB) based, air-stable, self-bleaching and easy-assembled solution-phase ECD, with an ITO/EC solution/ITO configuration without any adhesive sealing. This DPB-based ECD demonstrated outstanding color efficiency of 102.2 cm^2/C, and high ΔT of 72.2% at 517 nm under 1.8 V. In addition, ECDs can almost experience 5000 s (<5% degradation) of constant switching work with the electroactive solution exposure to air and moisture. This kind of ECDs possesses significant potential in smart windows, reflective products and other intelligent displays.

Declaration of competing interest

The authors declare no competing financial interest.

Acknowledgements

The authors would like to thank Shenzhen Fundamental Research Programs (JCYJ20170412152922553 and JCYJ20180305180635082), and the start-up fund of SUSTech (Y01256114), and the High-level university construction fund for SUSTech (G01256018).

Appendix A. Supplementary data

Supplementary data to this article can be found online at https://doi.org/10.1016/j.jelechem.2019.113447.

References

[1] H. Park, D.S. Kim, S.Y. Hong, C. Kim, J.Y. Yun, S.Y. Oh, S.W. Jin, Y.R. Jeong, G.T. Kim, J.S. Ha, A skin-integrated transparent and stretchable strain sensor with interactive color-changing electrochromic displays, Nanoscale 9 (2017) 7631–7640.

[2] R. Zheng, Y. Wang, C. Jia, Z. Wan, J. Luo, H.A. Malik, X. Weng, J. Xie, L. Deng, Intelligent biomimetic chameleon skin with excellent self-healing and electrochromic properties, ACS Appl. Mater. Interfaces 10 (2018) 35533–35538.

[3] J.W. Kim, J.M. Myoung, Flexible and transparent electrochromic displays with simultaneously implementable subpixelated ion gel-based viologens by multiple patterning, Adv. Funct. Mater. 29 (2019), 1808911.

[4] H. Oh, D.G. Seo, T.Y. Yun, C.Y. Kim, H.C. Moon, Voltage-tunable multicolor, sub-1.5 V, flexible electrochromic devices based on ion gels, ACS Appl. Mater. Interfaces 9 (2017) 7658–7665.

[5] Y. Alesanco, A. Vinuales, J. Palenzuela, I. Odriozola, G. Cabanero, J. Rodriguez, R. Tena-Zaera, Multicolor electrochromics: rainbow-like devices, ACS Appl. Mater. Interfaces 8 (2016) 14795–14801.

[6] B.J. Brownlee, M. Bahari, J.N. Harb, J.C. Claussen, B.D. Iverson, Electrochemical glucose sensors enhanced by methyl viologen and vertically aligned carbon nanotube channels, ACS Appl. Mater. Interfaces 10 (2018) 28351–28360.

[7] R. Celiesiute, A. Ramanaviciene, M. Gicevicius, A. Ramanavicius, Electrochromic sensors based on conducting polymers, metal oxides, and coordination complexes, Crit. Rev. Anal. Chem. 49 (2019) 195–208.

[8] J. Tong, X. Guo, L. Jia, X. Tian, A novel viologen-based visible and reversible paper sensor for oxygen, Mater. Lett. 158 (2015) 255–257.

[9] F. Sentanin, R.C. Sabadini, S.C. Barros, W.R. Caliman, C.C.S. Cavalheiro, J. Kanicki, J.P. Donoso, C.J. Magon, I.D.A. Silva, M.M. Silva, A. Pawlicka, Study of ionically conducting nanocomposites for reflective electrochromic devices, Electrochim. Acta 301 (2019) 174–182.

[10] K. Tajima, H. Hotta, Y. Yamada, M. Okada, K. Yoshimura, Electrochromic switchable mirror glass with controllable reflectance, Appl. Phys. Lett. 100 (2012), 091906.

[11] L. Yao, Z. Qu, Z. Pang, J. Li, S. Tang, J. He, L. Feng, Three-layered hollow nanospheres based coatings with ultrahigh-performance of energy-saving, antireflection, and self-cleaning for smart windows, Small 14 (2018), e1801661.

[12] H.C. Moon, T.P. Lodge, C.D. Frisbie, Solution Processable, electrochromic ion gels for sub-1 V, flexible displays on plastic, Chem. Mater. 27 (2015) 1420–1425.

[13] J. Palenzuela, A. Vinuales, I. Odriozola, G. Cabanero, H.J. Grande, V. Ruiz, Flexible viologen electrochromic devices with low operational voltages using reduced graphene oxide electrodes, ACS Appl. Mater. Interfaces 6 (2014) 14562–14567.

[14] E.O. Polat, O. Balci, C. Kocabas, Corrigendum: graphene based flexible electrochromic devices, Sci. Rep. 6 (2016), 18539.

[15] G.H. Santos, A.A.X. Gavim, R.F. Silva, P.C. Rodrigues, R.C. Kamikawachi, J.F. de Deus, A.G. Macedo, Roll-to-roll processed PEDOT:PSS thin films: application in flexible electrochromic devices, J. Mater. Sci. Mater. Electron. 27 (2016) 11072–11079.

[16] R. Singh, J. Tharion, S. Murugan, A. Kumar, ITO-free solution-processed flexible electrochromic devices based on PEDOT:PSS as transparent conducting electrode, ACS Appl. Mater. Interfaces 9 (2017) 19427–19435.

[17] X. Chen, H. Lin, J. Deng, Y. Zhang, X. Sun, P. Chen, X. Fang, Z. Zhang, G. Guan, H. Peng, Electrochromic fiber-shaped supercapacitors, Adv. Mater. 26 (2014) 8126–8132.

[18] W. Dong, Y. Lv, N. Zhang, L. Xiao, Y. Fan, X. Liu, Trifunctional NiO–Ag–NiO electrodes for ITO-free electrochromic supercapacitors, J. Mater. Chem. C 5 (2017) 8408–8414.

[19] R.T. Ginting, M.M. Ovhal, J.-W. Kang, A novel design of hybrid transparent electrodes for high performance and ultra-flexible bifunctional electrochromic-supercapacitors, Nano Energy 53 (2018) 650–657.

[20] Y. Guo, W. Li, H. Yu, D.F. Perepichka, H. Meng, Flexible asymmetric supercapacitors via spray coating of a new electrochromic donor-acceptor polymer, Adv. Energy Mater. 7 (2017), 1601623.

[21] S. Sathyamoorthi, M. Kanagaraj, M. Kathiresan, V. Suryanarayanan, D. Velayutham, Ethyl viologen dibromide as a novel dual redox shuttle for supercapacitors, J. Mater. Chem. A 4 (2016) 4562–4569.

[22] S. Tuukkanen, M. Valimaki, S. Lehtimaki, T. Vuorinen, D. Lupo, Behaviour of one-step spray-coated carbon nanotube supercapacitor in ambient light harvester circuit with printed organic solar cell and electrochromic display, Sci. Rep. 6 (2016), 22967.

[23] T. Ye, Y. Sun, X. Zhao, B. Lin, H. Yang, X. Zhang, L. Guo, Long-term-stable, solution-processable, electrochromic carbon nanotubes/polymer composite for smart

supercapacitor with wide working potential window, J. Mater. Chem. A 6 (2018) 18994–19003.

[24] T.Y. Yun, X. Li, S.H. Kim, H.C. Moon, Dual-function electrochromic supercapacitors displaying real-time capacity in color, ACS Appl. Mater. Interfaces 10 (2018) 43993–43999.

[25] P. Zhang, F. Zhu, F. Wang, J. Wang, R. Dong, X. Zhuang, O.G. Schmidt, X. Feng, Stimulus-responsive micro-supercapacitors with ultrahigh energy density and reversible electrochromic window, Adv. Mater. 29 (2017) 1604491.

[26] Y. Zhong, Z. Chai, Z. Liang, P. Sun, W. Xie, C. Zhao, W. Mai, Electrochromic asymmetric supercapacitor windows enable direct determination of energy status by the naked eye, ACS Appl. Mater. Interfaces 9 (2017) 34085–34092.

[27] G. Cai, J. Wang, P.S. Lee, Next-generation multifunctional electrochromic devices, Acc. Chem. Res. 49 (2016) 1469–1476.

[28] B. Gelinas, D. Das, D. Rochefort, Air-stable, self-bleaching electrochromic device based on viologen- and ferrocene-containing triflimide redox ionic liquids, ACS Appl. Mater. Interfaces 9 (2017) 28726–28736.

[29] S. Zhao, W. Huang, Z. Guan, B. Jin, D. Xiao, A novel bis(dihydroxypropyl) viologen-based all-in-one electrochromic device with high cycling stability and coloration efficiency, Electrochim. Acta 298 (2019) 533–540.

[30] T. Sakano, F. Ito, T. Ono, O. Hirata, M. Ozawa, T. Nagamura, Synthesis and electrochromic properties of a highly water-soluble hyperbranched polymer viologen, Thin Solid Films 519 (2010) 1458–1463.

[31] H.-S. Liu, B.-C. Pan, D.-C. Huang, Y.-R. Kung, C.-M. Leu, G.-S. Liou, Highly transparent to truly black electrochromic devices based on an ambipolar system of polyamides and viologen, NPG Asia Mater 9 (2017) e388.

[32] M. Li, D. Weng, Y. Wei, J. Zheng, C. Xu, Durability-reinforced electrochromic device based on surface-confined Ti-doped V_2O_5 and solution-phase viologen, Electrochim. Acta 248 (2017) 206–214.

[33] A. Danine, L. Manceriu, A. Fargues, A. Rougier, Eco-friendly redox mediator gelatin-electrolyte for simplified TiO2-viologen based electrochromic devices, Electrochim. Acta 258 (2017) 200–207.

[34] Y. Alesanco, A. Viñuales, J. Ugalde, E. Azaceta, G. Cabañero, J. Rodriguez, R. Tena-Zaera, Consecutive anchoring of symmetric viologens: electrochromic devices providing colorless to neutral-color switching, Sol. Energy Mater. Sol. Cells 177 (2018) 110–119.

[35] H. Oh, D.G. Seo, T.Y. Yun, S.B. Lee, H.C. Moon, Novel viologen derivatives for electrochromic ion gels showing a green-colored state with improved stability, Org. Electron. 51 (2017) 490–495.

[36] S. Abraham, S. Mangalath, D. Sasikumar, J. Joseph, Transmissive-to-black electrochromic devices based on cross-linkable tetraphenylethene-diphenylamine derivatives, Chem. Mater. 29 (2017) 9877–9881.

[37] R.J. Mortimer, T.S. Varley, Novel color-reinforcing electrochromic device based on surface-confined ruthenium purple and solution-phase methyl viologen, Chem. Mater. 23 (2011) 4077–4082.

[38] Y. Alesanco, A. Viñuales, G. Cabañero, J. Rodriguez, R. Tena-Zaera, Colorless-to-black/gray electrochromic devices based on single 1-alkyl-1′-aryl asymmetric viologen-modified monolayered electrodes, Adv. Opt. Mater. 5 (2017), 1600989.

[39] N. Jordão, H. Cruz, F. Pina, L.C. Branco, Studies of bipyridinium ionic liquids and deep eutectic solvents as electrolytes for electrochromic devices, Electrochim. Acta 283 (2018) 718–726.

[40] H.C. Lu, S.Y. Kao, H.F. Yu, T.H. Chang, C.W. Kung, K.C. Ho, Achieving low-energy driven viologens-based electrochromic devices utilizing polymeric ionic liquids, ACS Appl. Mater. Interfaces 8 (2016) 30351–30361.

[41] H. Tahara, K. Uranaka, M. Hirano, T. Ikeda, T. Sagara, H. Murakami, Electrochromism of ferrocene- and viologen-based redox-active ionic liquids composite, ACS Appl. Mater. Interfaces 11 (2019) 1–6.

[42] H. Tahara, R. Baba, K. Iwanaga, T. Sagara, H. Murakami, Electrochromism of a bipolar reversible redox-active ferrocene-viologen linked ionic liquid, Chem. Commun. 53 (2017) 2455–2458.

[43] Y. Rong, S. Kim, F. Su, D. Myers, M. Taya, New effective process to fabricate fast switching and high contrast electrochromic device based on viologen and Prussian blue/antimony tin oxide nano-composites with dark colored state, Electrochim. Acta 56 (2011) 6230–6236.

[44] D. Weng, Y. Shi, J. Zheng, C. Xu, High performance black-to-transmissive electrochromic device with panchromatic absorption based on TiO$_2$-supported viologen and triphenylamine derivatives, Org. Electron. 34 (2016) 139–145.

[45] M. Li, Y. Wei, J. Zheng, D. Zhu, C. Xu, Highly contrasted and stable electrochromic device based on well-matched viologen and triphenylamine, Org. Electron. 15 (2014) 428–434.

[46] E. Hwang, S. Seo, S. Bak, H. Lee, M. Min, H. Lee, An electrolyte-free flexible electrochromic device using electrostatically strong graphene quantum dot-viologen nanocomposites, Adv. Mater. 26 (2014) 5129–5136.

[47] K. Madasamy, D. Velayutham, V. Suryanarayanan, M. Kathiresan, K.-C. Ho, Viologen-based electrochromic materials and devices, J. Mater. Chem. C 7 (2019) 4622–4637.

[48] C.-R. Zhu, J.-F. Long, Q. Tang, C.-B. Gong, X.-K. Fu, Multi-colored electrochromic devices based on mixed mono- and bi-substituted 4,4′-bipyridine derivatives containing an ester group, J. Appl. Electrochem. 48 (2018) 1121–1129.

[49] G.K. Pande, N. Kim, J.H. Choi, G. Balamurugan, H.C. Moon, J.S. Park, Effects of counter ions on electrochromic behaviors of asymmetrically substituted viologens, Sol. Energy Mater. Sol. Cells 197 (2019) 25–31.

[50] D. Ma, G. Shi, H. Wang, Q. Zhang, Y. Li, Controllable growth of high-quality metal oxide/conducting polymer hierarchical nanoarrays with outstanding electrochromic properties and solar-heat shielding ability, J. Mater. Chem. A 2 (2014) 13541–13549.

[51] H.C. Moon, C.H. Kim, T.P. Lodge, C.D. Frisbie, Multicolored, low-power, flexible electrochromic devices based on ion gels, ACS Appl. Mater. Interfaces 8 (2016) 6252–6260.